



Characterization of alkali-treated cellulosic fibers derived from *Calamus tenuis* canes as a potential reinforcement for polymer composites

Arup Kar¹ · Dip Saikia² · Narayanasamy Pandiarajan³

Received: 22 January 2024 / Revised: 9 March 2024 / Accepted: 26 March 2024
© The Author(s), under exclusive licence to Springer-Verlag GmbH Germany, part of Springer Nature 2024

Abstract

This study evaluates the impact of a 4-h alkali treatment, using various concentrations of NaOH (2.5%, 5%, 7.5%, 10%, and 15% w/v), on *Calamus tenuis* cane fibers (CTCFs). Chemical analysis reveals a significant increase in cellulose content, reaching $50.07 \pm 1.67\%$ in CTCFs treated with 7.5% NaOH, accompanied by reductions in hemicellulose and lignin as confirmed by FTIR analysis. XRD analysis shows improved structural stability with an enhanced crystallinity index of $44.47 \pm 0.69\%$ and crystallite size of 3.03 ± 0.18 nm for CTCFs treated with 7.5% NaOH. TGA analysis indicates decreased activation energy and thermal stability post-treatment. Moreover, CTCFs treated with 7.5% NaOH exhibit peak values of Young's modulus (2.33 ± 0.05 GPa) and tensile strength (61.37 ± 1.05 MPa). SEM and AFM analyses confirm increased roughness post-treatment, enhancing fiber-matrix interlocking during composite fabrication. EDX analysis identifies an increased O/C ratio post-treatment, suggesting efficient removal of non-cellulosic elements. In conclusion, treating CTCFs with 7.5% NaOH for 4 h at ambient temperature enhances their physicochemical, structural, mechanical, and surface properties, indicating their potential for advanced polymer composites.

Keywords Alkali treatment · *Calamus tenuis* cane fibers · Cellulosic fibers · Morphological characteristics · Mechanical properties

1 Introduction

Over the last few decades, a notable surge has occurred in adopting natural fibers within the composite industries, driven by various compelling factors. The widespread use of these fibers is rooted in their abundant availability, eco-friendly origins, cost-effectiveness, lightweight characteristics, and impressive mechanical strength [1–3]. Additionally, natural fiber composites offer significant durability aspects that contribute to their growing popularity. These

composites exhibit remarkable resistance to fatigue, impact, and corrosion, making them suitable for prolonged usage in demanding applications across sectors such as construction materials, sports equipment, and automotive components [2, 4–6]. Researchers have meticulously examined and characterized a diverse array of natural fibers, including *Sansevieria trifasciata* [7], bark of *Rosa hybrida* [8], *Glycyrrhiza glabra* [9], *Raphia vinifera* [10], *Furcraea foetida* [11, 12], *Ficus religiosa* [13], and fragrant screw pine prop root [14]. The thorough studies on these materials not only emphasize their varied origins but also establish their suitability as reinforcement materials in the synthesis of composite structures. This exploration into natural fibers marks a crucial stride in sustainable materials, contributing significantly to the advancement of environmentally friendly and high-performance composites in diverse industrial sectors.

Plant fibers, primarily composed of cellulose, hemicellulose, and lignin, often display hydrophilic characteristics [15, 16]. Cellulose, a key constituent, imparts outstanding stability in structure, and resilience to these fibers [16]. Furthermore, the inclusion of lignin serves as a protective

✉ Dip Saikia
dr_dip_saikia@yahoo.co.in

¹ Department of Physics, Dibrugarh University, Dibrugarh 786004, Assam, India

² Department of Physics, Digboi College, Digboi 786171, Assam, India

³ Department of Mechanical Engineering, Kamaraj College of Engineering and Technology, Tamil Nadu, Madurai 625701, India

barrier against microbial attacks [2, 16]. Nevertheless, elevated levels of hemicellulose may have detrimental effects on natural fibers, leading to the degradation of fibers and a subsequent decline in mechanical properties [15]. Moreover, the hydrophilic properties pose difficulties in composite manufacturing, as these fibers show limited bonding with polymer matrices. This could potentially result in suboptimal mechanical characteristics in the produced composites [16]. Overcoming these challenges frequently requires the implementation of chemical modifications aimed at enhancing the bonding between matrix and fibers [17–19]. Various chemical treatments, including seawater treatment, acetylation, alkylation, NaOCl treatment, KMnO_4 treatment, HCl treatment, acetic acid (CH_3COOH) treatment, benzoyl peroxide ($\text{C}_{14}\text{H}_{10}\text{O}_4$) treatment, and silane treatment, have been explored for this purpose [16, 19–22]. Asma El Oudiani Ben Sghaier and her research team [23] investigated the influence of NaOCl and NaOH on the morphological and crystalline attributes of *Agave americana* L. fiber, demonstrating that optimizing NaOH concentration led to notable improvements in crystalline structure and morphological properties compared to NaOCl treatment. In a parallel study, Vijay and colleagues [24] explored *Pennisetum orientale* grass fibers, subjecting them to NaOH and HCl treatments, with results indicating superior crystalline and tensile properties with NaOH treatment over HCl treatment. Similarly, Mohammed and his fellow researchers [25] conducted a study on sugar palm fiber, utilizing 6% NaOH and varying concentrations of KMnO_4 for fiber-reinforced thermoplastic polyurethane composites. Their findings suggested that NaOH-treated sugar palm fiber-reinforced thermoplastic polyurethane composites exhibited superior flexural and thermal properties compared to KMnO_4 -treated counterparts. In summary, out of the range of chemical treatments investigated, treatment with alkali has proven to be the optimal and budget-friendly approach [23–26]. When subjected to alkali treatment with different concentrations, fibers undergo a transformative process, removing the non-cellulosic constituents from the fibers. This treatment will significantly enhance their mechanical properties and compatibility with polymer matrices, thereby establishing their viability as effective reinforcements in polymer composites. The improved characteristics resulting from this treatment are anticipated to positively influence the composite's structural integrity and performance, thereby offering a promising avenue for advanced material applications in the field of polysaccharides science [20].

Despite significant progress in various natural fibers, there remains a notable gap in the exploration of alkali treatment for *Calamus tenuis* cane fibers (CTCFs). Derived from the climbing palm tree called Jati Bet in Assam, India, these fibers are widely employed in North East India to produce

furniture, embellished items, and various products. Hence, the main focus of this research is to examine the effects of alkali treatment on fibers from *Calamus tenuis* canes (CTCFs). In this investigation, *Calamus tenuis* cane fibers (CTCFs) undergo treatments with varying concentrations of sodium hydroxide (NaOH)—specifically, 2.5% (w/v), 5% (w/v), 7.5% (w/v), 10% (w/v), and 15% (w/v)—each administered for 4 h at ambient temperature. Both untreated and treated samples undergo thorough analyses, encompassing chemical analysis, density and thickness measurements, X-ray diffraction (XRD) analysis, Fourier transformed infrared spectroscopy (FTIR) analysis, thermogravimetric analysis (TGA), energy dispersive X-ray spectroscopy (EDX) analysis, examination under a scanning electron microscope (SEM), atomic force microscope (AFM), and tensile test. This research aims to fill the existing gap in knowledge and contribute to the understanding of alkali treatment effects on CTCFs for potential applications in composite industries.

2 Materials and methods

2.1 Materials

Canes were harvested from the *Calamus tenuis* tree on the banks of the Burhi Dihing River in Naharkatia, Assam, India, situated at coordinates 27.2870° N, 95.2476° E. After extraction, a 14-day retting process was employed [27]. Following retting, the canes were subjected to a washing procedure using tap water. The canes were then subjected to an 8-day sun-drying period. Surface treatments were carried out using sodium hydroxide pellets (98% pure) sourced from Finar Limited, Ahmedabad, Gujarat.

2.2 Alkali treatment of fibers

The treatment of CTCFs involved the use of sodium hydroxide (NaOH) at varying concentrations, namely, 2.5% (w/v), 5% (w/v), 7.5% (w/v), 10% (w/v), and 15% (w/v) respectively as suggested by various researchers [28, 29], and was conducted at ambient temperature for 4 h. Thereafter, the canes were meticulously washed with distilled water to eliminate the remaining sodium hydroxide and then subjected to an 8-day sun-drying process.

2.3 Physical properties of CTCFs

The determination of density (ρ_b) for all samples adhered to the specifications provided in KSF 2198 [30, 31]:

$$\rho_b = \frac{W}{V} \quad (1)$$

In Eq. 1, W is the weight, and V signifies the volume of the samples.

The AM4113T Dino-Lite Digital USB Microscope-Pro manufactured by AnMo Electronics Corporation, Taiwan, was employed to estimate the thickness of the treated and untreated CTCFs.

2.4 Analysis of chemical compositions of CTCFs

Chemical composition analysis of all the samples of CTCFs was conducted following established protocols [32] to ascertain cellulose, hemicellulose, lignin, and ash content. The cellulose content was assessed utilizing the Updegraff method [33], which involves treating the sample with acetic-nitric reagent followed by selective removal of non-cellulosic components, ultimately leading to the hydrolysis of cellulose to glucose for quantification. For hemicellulose content determination, the neutral detergent fiber (NDF) method was applied [34], where the sample underwent treatment with neutral detergent to dissolve soluble components, leaving behind structural fibers including hemicellulose, which were quantified gravimetrically. Lignin content was quantified using the TAPPI T 222 om-02 standard method [32], involving acid digestion of the sample to solubilize lignin, followed by gravimetric analysis of the dissolved lignin. Furthermore, ash content was evaluated utilizing the TAPPI T 211 om-02 method [32], where the sample was incinerated at high temperatures to combust organic matter, and the remaining inorganic ash was quantified by weighing the residue. The chemical analyses were conducted thrice, and the reported results reflect the mean values.

2.5 Fourier transformed infrared (FTIR) analysis

The presence of functional groups in all samples of *Calamus tenuis* cane fibers (CTCFs) was examined by Fourier transformed infrared (FTIR) spectroscopy. The examination was carried out utilizing a Perkin Elmer 100 FT Spectrometer, USA, featuring 1 cm^{-1} resolution, spanning the wave number range from 400 to 4000 cm^{-1} .

2.6 X-ray diffraction (XRD) analysis

The examination of the crystalline properties of alkali-treated and untreated *Calamus tenuis* cane fibers (CTCFs) employed an Empyrean powder XRD, manufactured by PANalytical, UK, with a Cu X-ray tube serving as the X-ray source. The Cu X-ray tube, operating at a wavelength of 1.5418 \AA , featured a molybdenum (Mo) secondary monochromator to enhance the monochromaticity of the beam

of X-ray. Recordings of spectra were conducted across the 2θ range from 5 to 80° , employing a 0.026° step size. XRD analyses were performed with operational settings at a working voltage of 40 kV and a current of 40 mA , maintaining a temperature of 25°C . Segal's equation [35] was employed to determine the crystallinity index (CI) of alkali-treated and untreated CTCFs.

$$\text{CI} = \left(1 - \frac{I_{am}}{I_{002}} \right) \times 100\% \quad (2)$$

In Eq. 2, I_{002} represents the crystalline peak intensity. Conversely, I_{am} signifies the amorphous peak intensity.

The crystallite size (CS) of the samples was estimated employing Scherrer's equation [16].

$$\text{CS} = \frac{K\lambda}{\beta \cos\theta} \quad (3)$$

In Eq. 3, the symbol β denotes the FWHM of the peak, λ represents the X-ray wavelength, θ indicates Bragg's angle, and K stands for Scherrer's constant.

2.7 Thermogravimetric analysis (TGA)

Sample degradation properties were examined through a METTLER TOLEDO Thermogravimetric Analyzer, Model: TGA 2, New Castle, England. Both alkali-treated and untreated samples of CTCFs, 5 mg each, underwent heating from 25 to 700°C under a steady nitrogen flow at 20 mL/min . To estimate kinetic activation energy (E_a), the process involves plotting $\ln[-\ln(1-x)]$ along y-axis against $1000/T$ along x-axis using the Coats and Redfern equation [36].

$$\ln[-\ln(1-x)] = \ln \frac{ART^2}{\beta E_a} - \frac{E_a}{RT} \quad (4)$$

In Eq. 4, absolute temperature is represented by T , the pre-exponential factor is denoted by A , rate of heating is represented by β , gas constant is denoted by R , and $x = \frac{w_0 - w_t}{w_0 - w_f}$, where w_0 , w_t , and w_f denote the initial weight, weight at a specific time, and final weight of samples respectively.

2.8 Scanning electron microscopy (SEM) analysis and energy dispersive X-ray (EDX) spectroscopic analysis

The alkali-treated and untreated CTCFs were analyzed by JSM 6390LV Scanning Electron Microscope (SEM), JEOL, Japan, to analyze the morphology of the sample's surface. Before the analysis, the samples were subjected to gold coating. Elemental composition analysis of untreated and treated

CTCFs was performed using energy dispersive X-ray spectroscopy (Make: JOEL, Japan, Model: JSM-IT300).

2.9 Atomic force microscopy (AFM) analysis

Exploring the surface roughness of untreated and treated CTCFs involved employing an advanced three-dimensional visualization method through an atomic force microscope (AFM). The examination employed the NTEGRA Prima AFM, developed by NT-MDT Technology, Ireland. The samples were scanned using a Silicon cantilever at a frequency of 1 Hz. The investigation involved evaluating different parameters related to surface roughness, such as mean roughness (S_a), root mean square roughness (S_q or S_{rms}), maximum peak-to-valley height (S_p), ten points average absolute height roughness (S_z), kurtosis (S_{ku}), and surface skewness (S_{sk}).

2.10 Tensile test

The tensile properties of all treated and untreated *Calamus tenuis* canes were estimated using a universal testing machine (UTM) manufactured by INSTRON, Model: 8801, Massachusetts, outfitted with 100 kN as a load cell, at 24 °C. Testing involved 20 samples, utilizing a 50-mm gauge length and a 1-mm/min cross-head speed. The testing environment was consistently held at 55% RH during the entire procedure. Afterward, utilizing the Weibull distribution, an examination of the tensile characteristics parameters was conducted. The microfibril angle (α) for treated and untreated samples was calculated employing the following equation [37]:

$$\varepsilon = \ln\left(1 + \frac{\Delta L}{L_0}\right) = -\ln(\cos\alpha) \quad (5)$$

In Eq. 5, ε stands for strain, while gauge length is L_0 , and elongation at break is represented by ΔL , respectively, measured in millimeters.

3 Results and discussions

3.1 Physical properties of CTCFs

Equation 1 is used to ascertain the density of *Calamus tenuis* canes. Untreated samples display a density of $526 \pm 16 \text{ kg/m}^3$. Following treatment with 2.5%, 5%, 7.5%, 10%, and 15% NaOH, the density for CTCFs is increased by factors of 1.0038, 1.0057, 1.04, 1.055, and 1.0076, respectively. This surge in density is ascribed to the selective eradication of non-cellulosic components like pectin,

lignin, and hemicellulose leading to an increased cellulose content in the treated samples [13, 38]. Table 1 demonstrates that both alkali-treated and untreated CTCFs display diminished density compared to other plant fibers. For instance, their density is notably lower than that of alkali-treated *Ficus religiosa* (1272 kg/m^3) [13], alkali-treated Saharan aloe vera cactus leaves (1623.1 kg/m^3) [38], alkali-treated *Furcraea foetida* ($1347.52 \pm 39.3 \text{ kg/m}^3$) [11], alkali-treated *Agave americana* ($1041 \pm 22.68 \text{ kg/m}^3$) [39] and so on. The significantly low density of CTCFs is essential in the development of lightweight composites [2]. Simultaneously, the thickness of both untreated and treated CTCFs is assessed using an optical microscope. The measurements reveal a reduction in fiber thickness, decreasing from $0.5624 \pm 0.0272 \text{ mm}$ (untreated) to $0.5231 \pm 0.0365 \text{ mm}$, $0.4789 \pm 0.0268 \text{ mm}$, $0.4032 \pm 0.0098 \text{ mm}$, $0.3852 \pm 0.0450 \text{ mm}$, and $0.3474 \pm 0.0056 \text{ mm}$ for CTCFs treated with 2.5%, 5%, 7.5%, 10%, and 15% NaOH, respectively. The reduction in thickness is linked to the eradication of non-cellulosic constituents from the fibers' surface [13]. Figure 1 shows the optical microscope images of untreated and 7.5% NaOH-treated CTCFs.

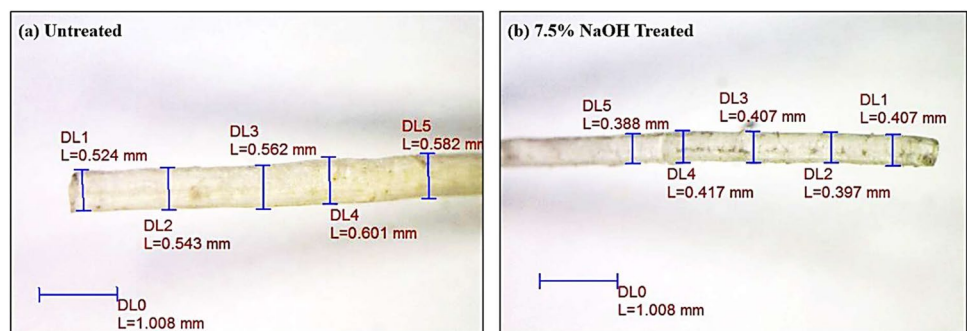
3.2 Analysis of chemical compositions of CTCFs

Exploring the effects of alkali treatment at varying concentrations on natural fiber, we conducted a detailed analysis of the key chemical constituents in both treated and untreated CTCFs [40, 41]. As evident from Table 1, the composition of the untreated CTCFs was presented with cellulose at $37.43 \pm 1.40\%$, hemicellulose at $31.06 \pm 1.03\%$, lignin at $28.42 \pm 0.81\%$, and a very small content of ash at $4.11 \pm 0.62\%$. Post-treatment, the lignin content, and the hemicellulose content are reduced as they are more susceptible to alkaline degradation than cellulose. Conversely, the cellulose being more resistant to alkaline degradation experienced a significant increase of 7.42%, 18.14%, 33.76%, 31.49%, and 24.97% for CTCFs treated with 2.5%, 5%, 7.5%, 10%, and 15% NaOH respectively; moreover, this increment also indicates the conversion of a small fraction of hemicellulose into natural cellulose [16, 42]. This heightened cellulose content holds the promise of substantially enhancing the thermal, crystalline, and mechanical properties of the plant fiber [2, 13]. Similar increments in cellulose content and decrements in hemicellulose content have been observed in various plant materials, such as *Ficus religiosa* [13], Saharan aloe vera cactus leaves [38], *Pongamia pinnata* L. bark [16], and *Pennisetum orientale* grass [24]. Additionally, Table 1 highlights a rise in ash content, signifying an enhancement in cellulose content in the CTCFs treated with alkali [41, 43].

Table 1 Comparison of physicochemical properties of alkali-treated and untreated CTCFs with other natural fibers

Fibers	Treatment	Physical properties		Chemical properties			
		Density (kg/m ³)	Thickness (mm)	Cellulose (%)	Hemicellulose (%)	Lignin (%)	Ash (%)
<i>Calamus tenuis</i> cane	Untreated [32]	526 ± 16	0.5624 ± 0.0272	37.43 ± 1.40	31.06 ± 1.03	28.42 ± 0.81	4.11 ± 0.62
	2.5% (w/v)	528 ± 19	0.5231 ± 0.0365	40.21 ± 1.21	29.07 ± 1.59	26.04 ± 1.01	4.66 ± 0.42
	5% (w/v)	529 ± 12	0.4789 ± 0.0268	44.22 ± 1.82	27.23 ± 1.27	23.17 ± 0.83	5.04 ± 0.78
	7.5% (w/v)	547 ± 11	0.4032 ± 0.0098	50.07 ± 1.67	23.36 ± 1.72	21.05 ± 1.11	5.28 ± 0.34
	10% (w/v)	555 ± 15	0.3852 ± 0.0450	49.22 ± 1.52	21.86 ± 1.38	20.62 ± 0.75	6.65 ± 0.64
	15% (w/v)	530 ± 10	0.3474 ± 0.0056	46.78 ± 1.08	20.85 ± 1.17	18.17 ± 1.18	7.84 ± 0.58
Saharan aloe vera cactus leaves [38]	Untreated	1325.1	0.09115	60.2	14.2	13.7	-
	5% (w/v)	1623.1	0.08061	67.4	8.2	13.7	-
Areca palm leaf stalk [2]	Untreated	1090 ± 24	0.285–0.330	57.49 ± 0.66	18.34 ± 0.24	7.26 ± 0.12	1.43 ± 0.019
	5% (w/v)	1170 ± 35	0.260–0.315	68.54 ± 0.72	6.13 ± 0.13	5.87 ± 0.20	1.10 ± 0.27
<i>Furcraea foetida</i> [11]	Untreated	1165.78 ± 52.2	0.3226 ± 0.0451	-	-	-	-
	9% (w/v)	1347.52 ± 39.3	0.2229 ± 0.0222	-	-	-	-
Corn husks [44]	Untreated	340	0.186 ± 0.02	46.15	33.79	3.92	-
	8% (w/v)	610	0.124 ± 0.02	62.87	13.62	5.55	-
<i>Pongamia pinnata</i> L. bark [16]	Untreated	1345	-	62.34	14.57	12.54	5.46
	5% (w/v)	1362	-	68.43	6.34	5.08	8.34
<i>Pennisetum orientale</i> grass [24]	Untreated	1045	0.2131	60.3	16	12.45	-
	5% (w/v)	1153	0.1795	66.7	10.3	8.7	-
Aerial roots of banyan tree [40]	Untreated	1234	0.00009–0.00014	67.32	13.46	15.62	3.96
	5% (w/v)	1269	0.00008–0.00012	70.4	10.74	10.74	5.86
<i>Thespesia populnea</i> bark [45]	Untreated	1412	0.16127 ± 0.0393	70.27	12.64	16.34	1.8
	5% (w/v)	1559	0.14632 ± 0.0896	76.42	9.59	12.78	1.96
<i>Coccinia grandis</i> L. [46]	Untreated	1243 ± 22.64	0.027 ± 0.003789	62.35	13.42	15.61	4.338
	5% (w/v)	1468 ± 34.32	0.025 ± 0.003014	68.47	8.64	11.32	7.845
Himalayan nettle [47]	Untreated	1420 ± 141	0.06669 ± 0.00348	90.39	5.64	2.41	-
	5% (w/v)	1550 ± 116	0.03484 ± 0.00149	92.53	4.32	1.72	-
<i>Cryptostegia grandiflora</i> [48]	Untreated	1020	0.117	79.2	17.2	2.5	3.2
	5% (w/v)	1470	0.108	82.6	12.1	1.5	2.4
<i>Tridax procumbens</i> [49]	Untreated	1160 ± 120	0.2331 ± 0.0099	32	6.8	3	-
	5% (w/v)	1350 ± 160	0.1697 ± 0.0092	45	3.6	2.1	-
Timoho fiber [50]	Untreated	760 ± 22	0.322613 ± 0.01664	37.05	14.68	17.18	-
	9% (w/v)	1020 ± 31	0.232491 ± 0.02284	42.75	10.31	24.65	-
Fragrant screw pine prop root [14]	Untreated	1385.2	-	73.1	12.58	7.11	-
	3% (w/v)	1410	0.121–0.343	80.53	7.45	5.24	-
<i>Zmioculus zamiifolia</i> [51]	Untreated	891 ± 17	0.33912 ± 0.01012	41.12 ± 3.32	10.14 ± 2.16	7.12 ± 2.17	-
	5% (w/v)	1113 ± 15	0.28635 ± 0.00985	52.63 ± 3.57	7.26 ± 1.24	4.12 ± 2.86	-

Fig. 1 Optical microscope images of **a** untreated CTCFs and **b** CTCFs treated with 7.5% NaOH



3.3 Fourier transformed infrared (FTIR) analysis

Table 2 displays the peak positions and their corresponding functional groups, clearly validating the existence of hemicellulose, cellulose, and lignin in both alkali-treated and untreated CTCFs. There exist ten unique absorption peaks at precise wavenumbers: 3419.69 cm^{-1} , 2928.04 cm^{-1} , 2848.42 cm^{-1} , 1738.71 cm^{-1} , 1634.37 cm^{-1} , 1507.25 cm^{-1} , 1375.10 cm^{-1} , 1247.05 cm^{-1} , 1072.22 cm^{-1} , and 898.07 cm^{-1} respectively.

The FTIR spectra of all the samples of CTCFs, as depicted in Fig. 2, exhibit remarkable similarity. Nevertheless, subtle differences exist in the FTIR spectra of the CTCFs subjected to the treatment with alkali. The significant, broad peak seen at 3419.69 cm^{-1} corresponds to vibrational stretching -OH group, signifying the existence of hydroxyl groups [45, 52–54] or α -cellulose [20, 42, 55]. Two moderate peaks positioned at 2928.04 cm^{-1} and 2848.42 cm^{-1} are indicative of the vibrational stretching of C-H bonds in cellulose and hemicellulose, respectively [56, 57]. A prominent peak at 1738.71 cm^{-1} was observed in the untreated fibers, resulting from the C=O group stretching and vibration, specifically associated with the presence of hemicellulose or lignin [37, 54]. After alkali treatment, this peak gradually diminishes and ultimately disappears, indicating the partial elimination of lignin and hemicellulose in the course of treatment with alkali [41, 54]. The detected peak at 1634.37 cm^{-1} indicates the presence of the C=O group in both lignin and hemicellulose [37]. A small peak positioned at 1507.25 cm^{-1} is indicative of the stretching of the C=C bond of aromatic lignin [24, 37, 58]. The peaks at 1375.10 cm^{-1} and 1247.05 cm^{-1} signify the bending of C-H groups within lignin and hemicellulose, respectively [52]. Following NaOH treatment, these peaks progressively diminish and eventually vanish, indicating the successful

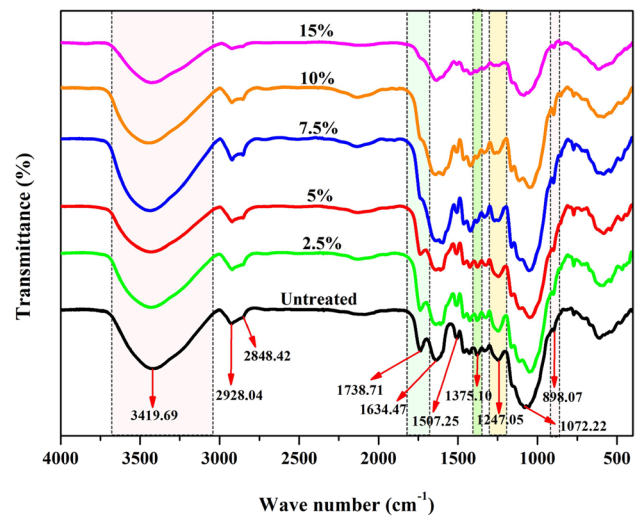


Fig. 2 FTIR spectra of alkali-treated and untreated CTCFs

eradication of lignin and hemicellulose [45]. The peak observed at 1072.22 cm^{-1} points to the presence of carbonyl groups of cellulose [37]. The peak noted at 898.07 cm^{-1} belongs to the C–O–C stretching within the β -glycosidic linkage of cellulose [53, 59]. Its intensity increases after 7.5% NaOH treatment, indicating cellulose's disrupted structure and transition from crystalline cellulose I to amorphous cellulose II [59].

3.4 X-ray diffraction (XRD) analysis

The XRD diagrams displayed in Fig. 3 reveal the presence of both crystalline and amorphous phases in the untreated and treated CTCF samples. In this analysis, the XRD pattern discloses the existence of three distinct crystalline planes, namely (101), (002), and (004), occurring

Table 2 Peak positions and the corresponding functional groups in alkali-treated and untreated CTCFs

Peak positions (wavenumbers (cm^{-1})) of untreated and treated CTCFs						Related functional groups and chemical constituents
Untreated CTCFs	2.5%	5%	7.5%	10%	15%	
3419.69	3419.69	3419.69	3419.69	3419.69	3419.69	OH-stretching vibrations of α -cellulose [20]
2928.04 and 2848.42	2928.04 and 2848.42	2928.04 and 2848.42	2928.04 and 2848.42	2928.04 and 2848.42	2928.04 and 2848.42	C-H stretching vibrations of cellulose and hemicellulose [24]
1738.71	1738.71	1738.71	-	-	-	C=O stretching vibrations of hemicellulose or lignin [24, 42]
1634.47	1634.47	1634.47	1634.47	1634.47	1634.47	C=O stretching of hemicellulose or lignin [16, 20]
1507.25	1507.25	1507.25	1507.25	1507.25	1507.25	C=C stretching vibration of aromatic lignin [24]
1375.10	1375.10	1375.10	1375.10	1375.10	-	C-H groups within lignin [52]
1247.05	1247.05	1247.05	1247.05	1247.05	-	C-H groups within hemicellulose [52]
1072.22	1072.22	1072.22	1072.22	1072.22	1072.22	C-O vibrations of cellulose [37]
898.07	898.07	898.07	898.07	898.07	898.07	C–O–C stretching of cellulose [53]

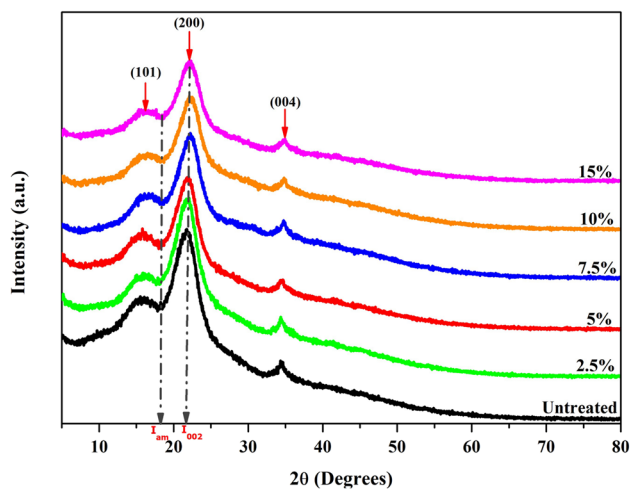


Fig. 3 XRD spectra of alkali-treated and untreated CTCFs

at approximately 2θ values of 16° , 22° , and 34.5° respectively [60, 61]. The diffraction peaks at around $2\theta = 16^\circ$ and 22° confirm the existence of cellulose I [48, 62–64], while the relatively weak peak at $2\theta = 34.5^\circ$ is assigned to the orientation and alignment of the fibers [42]. The trough at $2\theta = 18.11^\circ$ belongs to the non-crystalline section within the fiber [42]. The crystallinity index and crystallite size for both alkali-treated and untreated CTCFs are calculated using Eq. 2 and Eq. 3, respectively, and the resulting values are displayed in Table 3. From Table 3, it is observed that the untreated samples display a crystallinity value of $37.38 \pm 0.27\%$. The crystallinity index value exhibits an increment with the rise in NaOH concentration, reaching its peak at 7.5% NaOH treatment, where it attains a value of $44.47 \pm 0.69\%$. However, treatment with 10% and 15% NaOH leads to a reduction in the crystallinity index, yielding values of $43.55 \pm 0.57\%$ and $42.16 \pm 0.83\%$, respectively. The enhancement in the crystallinity index is ascribed to the elimination of non-crystalline and amorphous constituents from the fibers which subsequently boosts the prevalence of crystalline cellulose [21, 52, 54]. On the contrary, the primary reason for the reduction in the crystallinity index may be the conversion of cellulose I to cellulose II [59, 65]. The crystallinity index values for both treated and untreated samples CTCFs are significantly greater than those of *Penisetum orientale* grass (33.5%) [24], *Mucuna atropurpurea* (24.01%) [43], *Tridax procumbens* (34.46%) [49], and *Draecena draco* (30.42%) [66] while they are smaller than those of Saharan aloe vera cactus leaves (52.6%) [38], *Furcraea foetida* (62.05%) [11], *Himalayacalamus falconeri* culms (58.92%) [42], and so forth. Furthermore, Table 3 also illustrates that when CTCFs are treated with 7.5% NaOH, there is a noticeable growth in crystallite size, progressing from 2.73 ± 0.12 nm to 3.03 ± 0.18 nm. The increase in crystallite size is advantageous as it influences the moisture absorption

characteristics of plant fibers [16, 24, 38]. The untreated and treated CTCFs exhibit crystallite sizes higher than those of *Furcraea foetida* (2.44 nm) [11], corn husks (2.25 nm) [44], and *Mucuna atropurpurea* (2.75 nm) [43], while they are smaller than the crystallite sizes observed in *Ficus religiosa* (5.18 nm) [13], *Pongamia pinnata* L. bark (5.43 nm) [16], *Phaseolus vulgaris* (4.07 nm) [41], among others.

3.5 Thermogravimetric analysis (TGA)

Figure 4a and b display the TGA and DTG curves for alkali-treated and untreated CTCFs, illustrating a clearly defined three-stage degradation process. These weight loss patterns at each stage are succinctly summarized in Table 4.

The data in Table 4 reveals that a minor weight loss, roughly between 13 and 18%, occurs between 25 and 125°C , primarily attributed to the evaporation of moisture [54, 69, 70]. The most significant weight loss, approximately 49 to 54%, is observed between 190 and 350°C . Within this temperature range, the DTG curve of untreated CTCFs exhibits two distinct peaks: one at approximately 292.41°C , which belongs to the breakdown of glycosidic links in cellulose, hemicellulose, and pectin [71], and the other at 316.23°C , attributed to the degradation of α -cellulose [62, 72]. Notably, the treated CTCFs display only a single peak, indicative of the successful removal of hemicellulose during alkali treatment. Furthermore, it is worth noting that the cellulose degradation temperature shifts toward lower temperatures after treatment, suggesting a decrease in thermal stability. The precise cause of this reduced thermal stability is not fully understood in this study, but it may involve alterations in crystallinity or changes in cellulose chain structures [69, 70]. Conversely, other sources propose that the decrease in thermal stability may result from the reduction of amorphous regions within the fibers [73, 74]. The thermal stability of both alkali-treated and untreated CTCFs closely approaches that of *Furcraea foetida* (204.04°C) [11] and *Mucuna atropurpurea* (200°C) [43]. However, it falls short of the levels observed in *Himalayacalamus falconeri* culms (250°C) [42], Areca palm leaf stalk (279°C) [2], and Saharan aloe vera cactus leaves (225°C) [38]. Lignin is the final component in natural fibers to undergo degradation, taking place in the last stage (350 to 700°C) [65, 75]. At a temperature of 700°C , the remaining weights are recorded at 0.045% for untreated CTCFs and 0.28%, 0.08%, 0.037%, 0.39%, and 0.066% for treated CTCFs, respectively. Upon analyzing Fig. 4c, we conducted the assessment of kinetic activation energy for both treated and untreated samples. The estimation of kinetic activation energy is crucial for examining the degradation processes and thermal stability of natural fibers. The analysis revealed that untreated CTCFs exhibit a kinetic activation energy of 59.28 kJ/mol. In contrast, the treated fibers demonstrate a lower kinetic activation energy

Table 3 Comparison of structural, thermal, and mechanical properties of alkali-treated and untreated CTCFs with other natural fibers

Fibers	Treatment	Structural properties		Thermal properties		Mechanical properties			
		CrI (%)	CS (nm)	Thermal stability (°C)	Maximum degradation temperature (°C)	Tensile strength (MPa)	Young's modulus (GPa)	Elongation at break (%)	Microfibril angle (°)
<i>Calamus tenuis</i> cane [32]	Untreated	37.38 ± 0.27	2.73 ± 0.12	215 ± 5	316.23	37.5 ± 2	1.05 ± 0.08	18.94 ± 4.26	34.22 ± 6.44
	2.5% (w/v)	41.36 ± 0.46	2.84 ± 0.21	192 ± 4	293.70	40.11 ± 1.57	1.25 ± 0.07	16.67 ± 2.4	33.57 ± 4.07
	5% (w/v)	41.55 ± 0.19	2.96 ± 0.09	199 ± 2	292.48	47.38 ± 1.12	1.3 ± 0.06	12.77 ± 3	29.27 ± 1.56
	7.5% (w/v)	44.47 ± 0.69	3.03 ± 0.18	195 ± 8	287.48	61.37 ± 1.05	2.33 ± 0.05	8.41 ± 1.92	23.17 ± 1.98
	10% (w/v)	43.55 ± 0.57	2.89 ± 0.13	192 ± 5	291.62	38.63 ± 1.01	1.33 ± 0.04	12.61 ± 2.36	28.38 ± 1.58
Saharan aloe vera cactus leaves [38]	Untreated	52.6	5.6	225	350	621.8	40.03	2.47	11.1
	5% (w/v)	56.5	5.72	231	355	805.5	42.29	2.39	10.3
Areca palm leaf stalk [2]	Untreated	-	-	279	365	334.66 ± 21.46	7.64 ± 1.13	4.38 ± 1.15	-
	5% (w/v)	-	-	285	368	486.41 ± 35.57	9.89 ± 1.46	4.91 ± 1.82	-
<i>Furcraea foetida</i> [11]	Untreated	62.05	2.44	204.04	356.75	192.37 ± 21.45	7.45 ± 1.31	4.51 ± 0.73	17.09
	9% (w/v)	74.35	4.15	231.11	358.78	416.11 ± 39.11	12.36 ± 1.68	8.34 ± 0.50	23.07
<i>Ficus religiosa</i> [13]	Untreated	42.92	5.18	-	325	421.25 ± 18	5.11 ± 1.4	9.21 ± 2.3	-
	5% (w/v)	48.64	6.74	-	356	530.3 ± 23.70	8.02 ± 1.12	6.60 ± 0.53	-
Corn husks [44]	Untreated	43.73	2.25	-	-	160.49 ± 17.12	4.57 ± 0.54	21.08 ± 2.86	-
	8% (w/v)	59.49	3.16	-	-	368.25 ± 78.97	15.87 ± 1.87	7.41 ± 0.61	-
<i>Pongamia pinnata</i> L. bark [16]	Untreated	45.31	5.43	-	332	322 ± 16.10	9.67 ± 0.144	2.09 ± 0.214	-
	5% (w/v)	52.43	8.32	-	348	343.6 ± 13.04	12.71 ± 0.132	1.98 ± 0.145	-
<i>Dichro- tachys cinerea</i> bark [20]	Untreated	57.82	-	-	359.3	820 ± 10	70.6	10 ± 3	-
	5% (w/v)	65.63	-	-	370.3	855 ± 10	72.25	18 ± 2	-
Aerial roots of banyan tree [40]	Untreated	72.47	6.28	230	358	19.37 ± 7.72	1.8 ± 0.40	1.8 ± 0.40	10.88 ± 1.198
	5% (w/v)	76.35	7.74	230	368	20.45 ± 12.20	0.82 ± 0.32	1.6 ± 0.50	10.17 ± 1.587
<i>Phaseolus vulgaris</i> [41]	Untreated	43.01	4.07	-	322.1	436 ± 10.1	8.98 ± 1.237	1.48 ± 0.03	-
	5% (w/v)	52.27	8.25	-	346.6	523 ± 10.6	10.64 ± 1.53	1.63 ± 0.03	-
<i>Himalaya- calamus falconeri</i> culms [42]	Untreated	58.92	3.39	250	356.25	132	10.26	1.3	-
	5% (w/v)	67.79	3.8	258	361.78	196.5	19.61	1.23	-
<i>Mucuna atropur- purea</i> [43]	Untreated	24.01	2.75	200	298	274.6 ± 29.5	2.88 ± 1.026	2.208 ± 0.654	11.87 ± 1.72
	5% (w/v)	49.89	1.6	200	320	307.3 ± 24.12	4.633 ± 0.94	1.776 ± 0.56	10.64 ± 1.65
<i>Perotis indica</i> [67]	Untreated	48.3	15.12	-	329.35	32.3	69.61	-	8.45–15.87
	5% (w/v)	55.43	18.51	-	348.78	34.9	79.45	-	-
<i>Thespesia populnea</i> bark [45]	Untreated	48.17	-	-	323.76	557.82 ± 56.29	20.57 ± 4.46	2.80 ± 0.56	13.94 ± 1.21
	5% (w/v)	67.52	-	-	341.82	678.41 ± 48.91	22.73 ± 4.18	3.14 ± 0.39	14.51 ± 1.28
<i>Coccinia grandis</i> L. [46]	Untreated	52.17	13.38	213.4	351.6	273 ± 27.74	10.17 ± 1.261	2.703 ± 0.2736	13.25 ± 0.6641
	5% (w/v)	56.64	8.15	220.6	360.1	316.3 ± 36.63	14.29 ± 2.874	2.258 ± 0.2834	12.11 ± 0.7661
Himalayan nettle [47]	Untreated	75.5	11.11	297	362.62	158.23 ± 10.6	35.32 ± 19.39	1.70 ± 0.35	10.47 ± 1.04
	5% (w/v)	79.1	5.2	311	353.69	296.97 ± 158.96	36.27 ± 16.99	1.84 ± 0.37	10.87 ± 1.06
<i>Tridax procum- bens</i> [49]	Untreated	34.46	25.04	195	250, 330	25.75	0.94 ± 0.09	2.77 ± 0.27	13.4 ± 0.64
	5% (w/v)	40.85	38.23	223	280	33.62	1.5 ± 0.27	2.30 ± 0.32	12.21 ± 0.85

Table 3 (continued)

Fibers	Treatment	Structural properties		Thermal properties		Mechanical properties			
		CrI (%)	CS (nm)	Thermal stability (°C)	Maximum degradation temperature (°C)	Tensile strength (MPa)	Young's modulus (GPa)	Elongation at break (%)	Microfibril angle (°)
<i>Abelmoschus ficulneus</i> weed [68]	Untreated	56.25	4.17	-	349.83	538	0.128	2.57 ± 1.29	-
	5% (w/v)	60.46	5.84	-	352.33	1292	0.159	1.65 ± 0.40	-
Fragrant screw pine prop root [14]	Untreated	-	21.96	-	321.4	531–915	21–33	3.36–8.85	-
	3% (w/v)	64.8	25.71	-	341.8	619–1038	23–41	3.84–9.91	-
<i>Zmioculus zamiiifolia</i> [51]	Untreated	25.75 ± 2.34	2.54 ± 0.24	310.32 ± 1.32	361.13 ± 2.54	34.92 ± 5.47	0.136 ± 0.052	-	-
	5% (w/v)	37.80 ± 4.57	4.16 ± 0.62	326.82 ± 2.45	367.11 ± 2.61	48.25 ± 5.49	0.240 ± 0.039	-	-

when compared to their untreated counterparts. Specifically, the kinetic activation energies for fibers treated with 2.5%, 5%, 7.5%, 10%, and 15% NaOH were measured at 47.42 kJ/mol, 49.58 kJ/mol, 51.08 kJ/mol, 58.32 kJ/mol, and 57.99 kJ/mol, respectively.

3.6 Scanning electron microscopy (SEM) analysis and energy dispersive X-ray (EDX) spectroscopic analysis

The SEM pictures depicted in both Fig. 5 and Fig. 6 provide a visual representation that highlights the differences between treated and untreated CTCFs. Specifically, Fig. 5 offers a cross-sectional perspective of untreated and treated CTCFs, unveiling their composition, which includes metaxylem (characterized by large-sized pores), protoxylem, phloem, dark grey-colored parenchyma cells, and a fibrous sheath [76–78]. An intriguing aspect emerges from the analysis, revealing a notable alteration in the cross-sectional pattern after treatment. Following the treatment, a transformative process takes place as lignin, hemicellulose, pectin, and wax are removed from the fibers' surface. This removal results in a decrease in the size of the metaxylem, and concurrently, the destruction of cells between the cell walls occurs, leading to their fusion with neighboring cells [79]. In Fig. 6, the untreated fibers display a sleek texture primarily attributed to the existence of diverse impurities and other non-cellulosic elements [38, 44]. However, when subjected to NaOH treatment at varying concentrations, a substantial transformation occurs in the fiber surface, as discerned from the SEM images shown in Fig. 6 (ranging from 2.5 to 15%). This treatment is notably effective in removing impurities and other non-cellulosic constituents [44, 62], leading to a visibly roughened surface texture [48]. Additionally, the alkali treatment can cause swelling of the CTCFs, leading to an increase in surface area and roughness [80]. This

swelling is due to the penetration of alkali solution to the fiber structure, causing the cellulose chains to separate and enlarge. Consequently, this swelling effect can contribute to the roughening of the fiber surface. The heightened surface area of the fibers enhanced the adhesion and bonding between fibers and the matrix, thereby improving overall mechanical properties [80]. Furthermore, the increased irregularities create mechanical interlocking, facilitating better load transfer between fibers and the matrix, leading to improved strength and stiffness of the composite material [2, 38]. This enhancement in roughness stands out as a critical factor contributing to the altered surface characteristics of the treated fibers, thereby influencing their interactions and compatibility with the surrounding material matrix [81].

Figure 7 provides visual representations of the EDX spectrum, revealing the presence of various elements dispersed on the outer surface of untreated and treated CTCFs. Within Fig. 7, it is evident that oxygen (O) and carbon (C) are the predominant elements found in both treated and untreated CTCFs. In untreated CTCFs, the higher carbon (C) content serves as a clear indicator of a more significant presence of lignin [82]. Post-treatment, the reduction in carbon content indicates the partial removal of lignin. The most notable observation is the CTCFs treated with 2.5%, 5%, 7.5%, 10%, and 15% NaOH, displaying the highest oxygen-to-carbon ratio of 1.59%, 1.61%, 1.77%, 1.52%, and 1.76% respectively. This ratio signifies the effective removal of lignin and hemicellulose, along with an increase in cellulose content [82, 83]. Additionally, it is worth noting that both untreated and treated CTCFs contain certain contaminants such as magnesium (Mg), calcium (Ca), and silicon (Si). Furthermore, untreated CTCFs exhibit a sodium (Na) content of only 0.67%. However, after alkali treatment, the sodium (Na) content increases as compared to the untreated one, indicating the deposition of some sodium (Na) during the treatment process [16, 42].

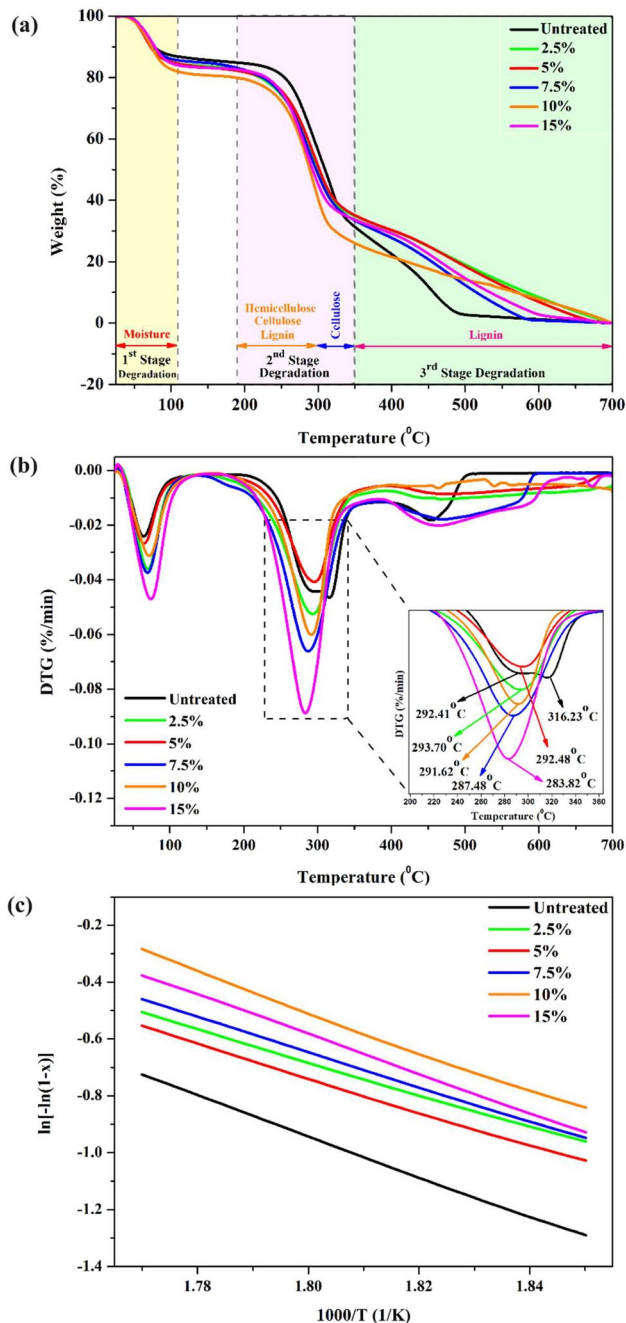


Fig. 4 a TGA graph, b DTG graph, and c graph for the estimation of kinetic activation energy of alkali-treated and untreated CTCFs

3.7 Atomic force microscopy (AFM) analysis

Figure 8 presents 3D topographic visualizations and surface roughness parameters for alkali-treated and untreated CTCFs. Examination of the 3D AFM images reveals a discernible rise in surface roughness post-treatment. The average roughness (S_a) of untreated CTCFs measures 88.1 nm, whereas post-treatment values escalate to 104.6 nm, 114.2 nm, 135.3 nm, 152.6 nm, and 182 nm, respectively.

Similar increases in average roughness (S_a) values have been observed in various other natural fibers. For instance, the Areca palm leaf stalk shows an increase from 0.694 to 0.790 nm [2], *Himalayacalamus falconeri* culms demonstrate an escalation from 23.478 to 37 nm [42], and *Mucuna atropurpurea* displays a growth from 27.113 to 77.373 nm [43], among others. This enhanced roughness is linked to the elimination of contaminations and non-cellulosic elements from the outer surface of the fibers [16, 42]. The treated CTCFs exhibit negative surface skewness (S_{sk}), signifying the porous characteristics of the fibers' surface [43, 67]. Additionally, the reduction in surface kurtosis (S_{ku}) values from 3.335 (for untreated CTCFs) to 3.1765, 3.1055, 2.896, 2.718, and 1.128 for CTCFs treated with 2.5%, 5%, 7.5%, 10%, and 15% NaOH, respectively, signifies increased surface roughness post-treatment [16, 43]. Improvement in other roughness parameters such as S_p , S_z , and S_q is also observed after treatment. The results suggest that alkali treatment enhances the surface roughness of the fibers, facilitating better interlocking between the matrix and the fibers during the fabrication of polymer composites [2, 38].

3.8 Tensile test

Figure 9a and b illustrate the stress–strain curve and tensile characteristics of all the samples of treated and untreated CTCFs, respectively. Examination of the stress–strain curve reveals that untreated CTCFs exhibit a tensile strength value of 37.5 ± 2 MPa, 1.63 times lower than that of the CTCFs treated with 7.5% NaOH, measuring 61.37 ± 1.05 MPa. This measurement surpasses the tensile strength of alkali-treated fibers from various sources, including aerial roots of the banyan tree (20.45 ± 12.20 MPa) [40], *Perotis indica* (34.9 MPa) [67], and *Tridax procumbens* (33.62 MPa) [49]. Post-treatment, there are noteworthy changes in other parameters, including elongation at break and Young's modulus. Young's modulus increases to 2.33 ± 0.05 GPa for the CTCFs treated with 7.5%, a substantial rise from the 1.05 ± 0.08 GPa observed in untreated CTCFs. A comparison with values in Table 3 reveals that the Young's modulus of 7.5% NaOH-treated CTCFs far exceeds that of alkali-treated fibers from aerial roots of the banyan tree (0.82 ± 0.32 GPa) [40], *Tridax procumbens* (1.5 ± 0.27 GPa) [49], and *Abelmoschus ficulneus* Weed (0.159 GPa) [68]. Simultaneously, elongation at break decreases from $18.94 \pm 4.26\%$ (for untreated CTCFs) to $8.41 \pm 1.92\%$ (for 7.5% treated CTCFs). The augmentation in tensile strength and Young's modulus values is ascribed to the extraction of non-cellulosic elements such as lignin, hemicellulose, and other waxy substances from the fibers [1, 38, 51]. This process is complemented by enhancements in the crystallinity index through alkali treatment, thereby yielding improved mechanical properties [1]. Moreover, the creation of fresh hydrogen bonds among cellulose fibrils

Table 4 Thermal degradation characteristics of alkali-treated and untreated CTCFs

<i>Calamus tenuis</i> cane fibers	1st stage of decomposition			2nd stage of decomposition			3rd stage of decomposition		
	Temp. range (°C)	Peak temp. (°C)	Wt. loss (%)	Temp. range (°C)	Peak temp. (°C)	Wt. loss (%)	Temp. range (°C)	Peak temp. (°C)	Wt. loss (%)
Untreated	25 to 125	64.39	13.03	190 to 350	316.23	53.53	350 to 700	453.94	31.32
					292.41				
2.5%	25 to 125	70.01	15.27	190 to 350	293.70	47.60	350 to 700	-	34.82
5%	25 to 125	65.37	15.33	190 to 350	292.48	48.07	350 to 700	-	35.10
7.5%	25 to 125	69.66	14.36	190 to 350	287.48	49.68	350 to 700	-	33.38
10%	25 to 125	72.16	18.21	190 to 350	291.62	53.79	350 to 700	-	26.04
15%	25 to 125	74.28	15.84	190 to 350	283.82	49.00	350 to 700	-	33.66

and the development of densely packed structures within the fiber collectively contribute to the enhanced mechanical characteristics of the CTCFs [1, 51]. Nevertheless, when NaOH concentrations are increased to 10% and 15%, both tensile strength and Young's modulus values experience a decline. This occurrence is linked to the destructive effect of high NaOH concentrations on cementing materials such as hemicellulose and other waxy substances [47, 65]. Additionally, it impacts cellulose fibrils, resulting in fiber weakening and a subsequent decrease in fiber stiffness [65]. The microfibril angle (MFA) of both treated and untreated CTCFs was determined using Eq. 5. The MFA for 7.5% NaOH-treated CTCFs is measured at $23.17 \pm 1.98^\circ$, lower than the MFA of untreated CTCFs ($34.22 \pm 6.44^\circ$). This value closely aligns with the MFA values of alkali-treated fibers from *Furcraea foetida* (23.07°) [11], coir (30.45°) [84], Rachilla ($35\text{--}39^\circ$) [84], and others. Natural fibers with higher MFA demonstrate greater flexibility and ductility properties, as the microfibril angle directly correlates with applied strain [46, 47]. Conversely, fibers with a lower MFA exhibit superior stiffness and mechanical properties, as MFA inversely influences Young's modulus and tensile strength [46, 47]. The Weibull distribution plot for tensile strength, Young's modulus, elongation at break, and microfibril angle is presented in Fig. 10, affirming the alignment of all parameters along the line and their excellent conformity to the Weibull distribution.

4 Conclusions

This comprehensive study meticulously explores the diverse properties of treated and untreated CTCFs, encompassing physio-chemical, structural, thermal, mechanical, and morphological aspects. Chemical analysis reveals that the cellulose content for untreated CTCFs is $37.43 \pm 1.40\%$, with a notable increase to a maximum of $50.07 \pm 1.67\%$

post-treatment with 7.5% NaOH. Simultaneously, there is a substantial reduction in hemicellulose and lignin content. Despite an increase in density after treatment, CTCFs maintain a lower density compared to other natural and synthetic fibers, establishing their suitability for lightweight composite applications. FTIR spectra confirm the effective eradication of lignin and hemicellulose. XRD analysis demonstrates a significant enhancement in crystallinity index and crystallite size after treatment, reaching peaks of $44.47 \pm 0.69\%$ and 3.03 ± 0.18 nm, respectively, with 7.5% NaOH treatment. This indicates that the treatment, particularly at these specific NaOH concentrations, significantly elevates the fibers' crystallinity, potentially augmenting overall structural stability and strength. TGA analysis reveals a reduction in thermal stability post-treatment, yet the treated samples maintain average stability up to $195 \pm 5^\circ\text{C}$, making them suitable for reinforcement in high-temperature applications. Tensile strengths and Young's modulus experience substantial improvement, increasing from 37.5 ± 2 MPa and 1.05 ± 0.08 GPa to 61.37 ± 1.05 MPa and 2.33 ± 0.05 GPa, respectively, for CTCFs treated with 7.5% NaOH, while the elongation at break decreases from $18.94 \pm 4.26\%$ (for untreated) to $8.41 \pm 1.92\%$ (for CTCFs treated with 7.5% NaOH). Microscopic investigations employing SEM and AFM illustrate a surface with a pronounced rough texture, indicating the extraction of hemicellulose, pectin, and lignin. EDX analysis confirms that treatment with different concentrations of NaOH increases the O/C ratio, signifying the efficient eradication of non-cellulosic constituents post-treatment. In summary, treating CTCFs with 7.5% NaOH at ambient temperature for 4 h significantly enhances their physical, chemical, structural, mechanical, and surface characteristics. The simultaneous decrease in lignin and hemicellulose content, along with a rise in cellulose percentage, positions these fibers as exceptionally promising contenders for advanced polymer composite materials.

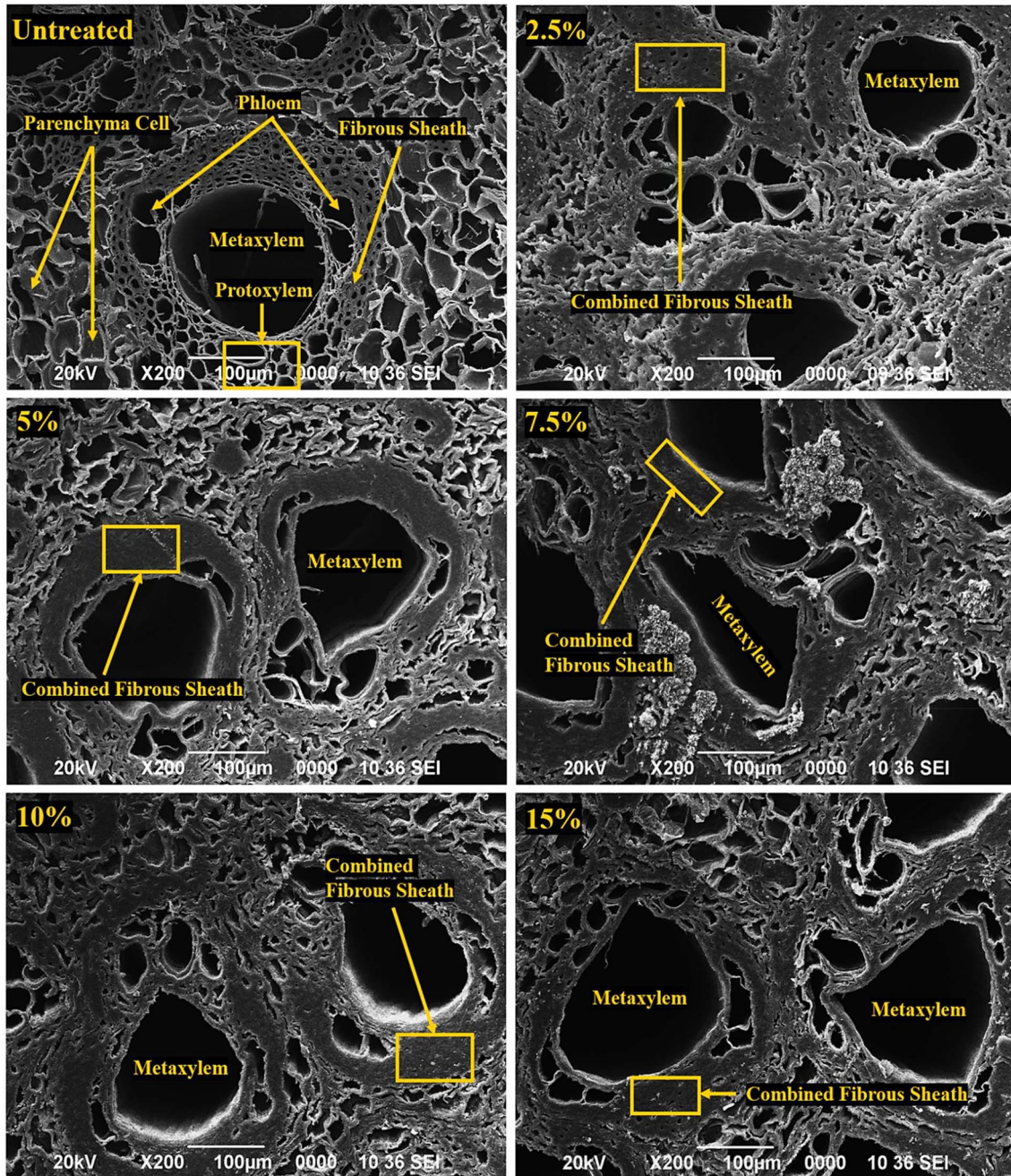


Fig. 5 SEM images of the cross-section of alkali-treated and untreated CTCFs

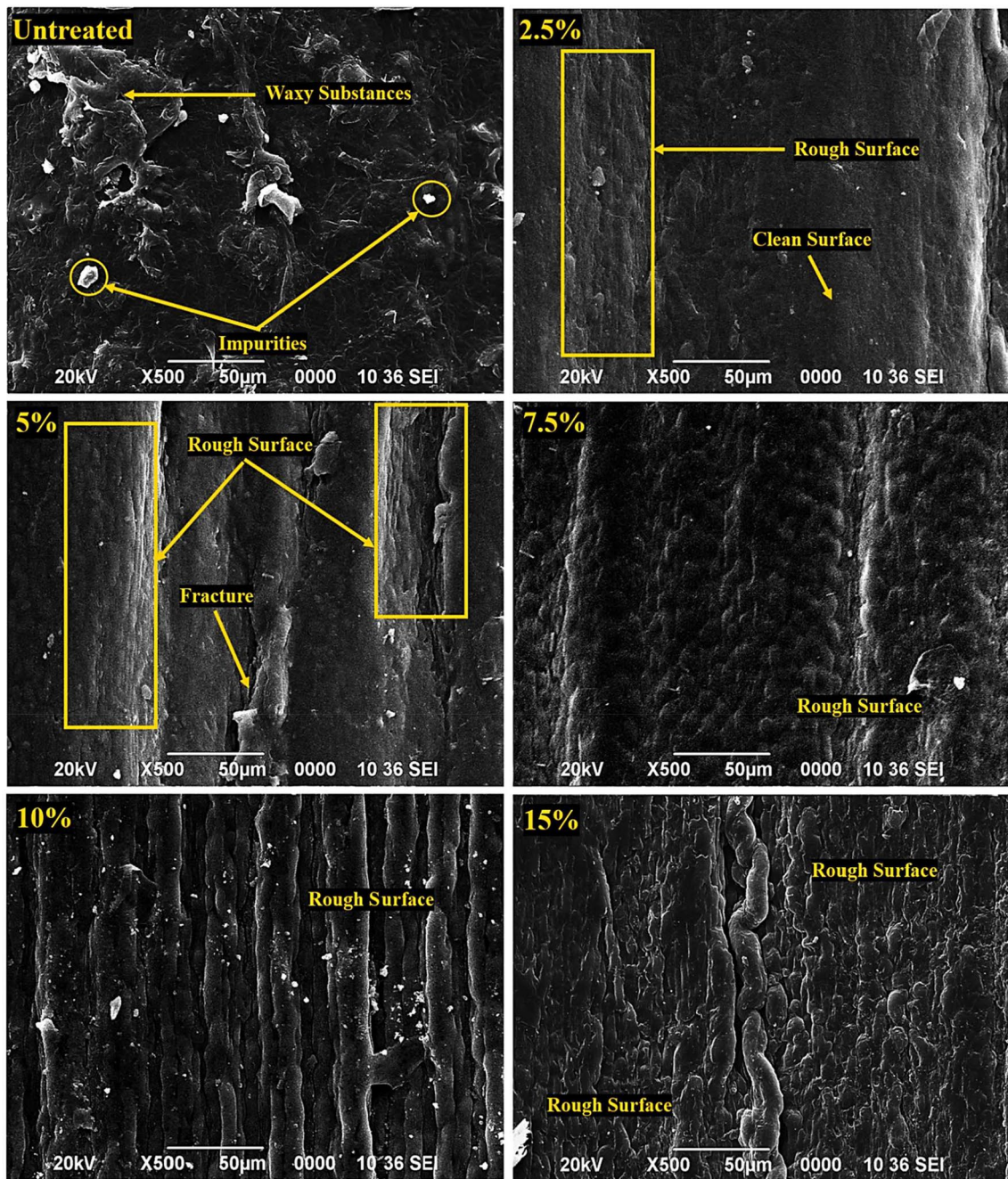


Fig. 6 SEM images of the longitudinal section of alkali-treated and untreated CTCFs

Fig. 7 EDX spectrum of alkali-treated and untreated CTCFs

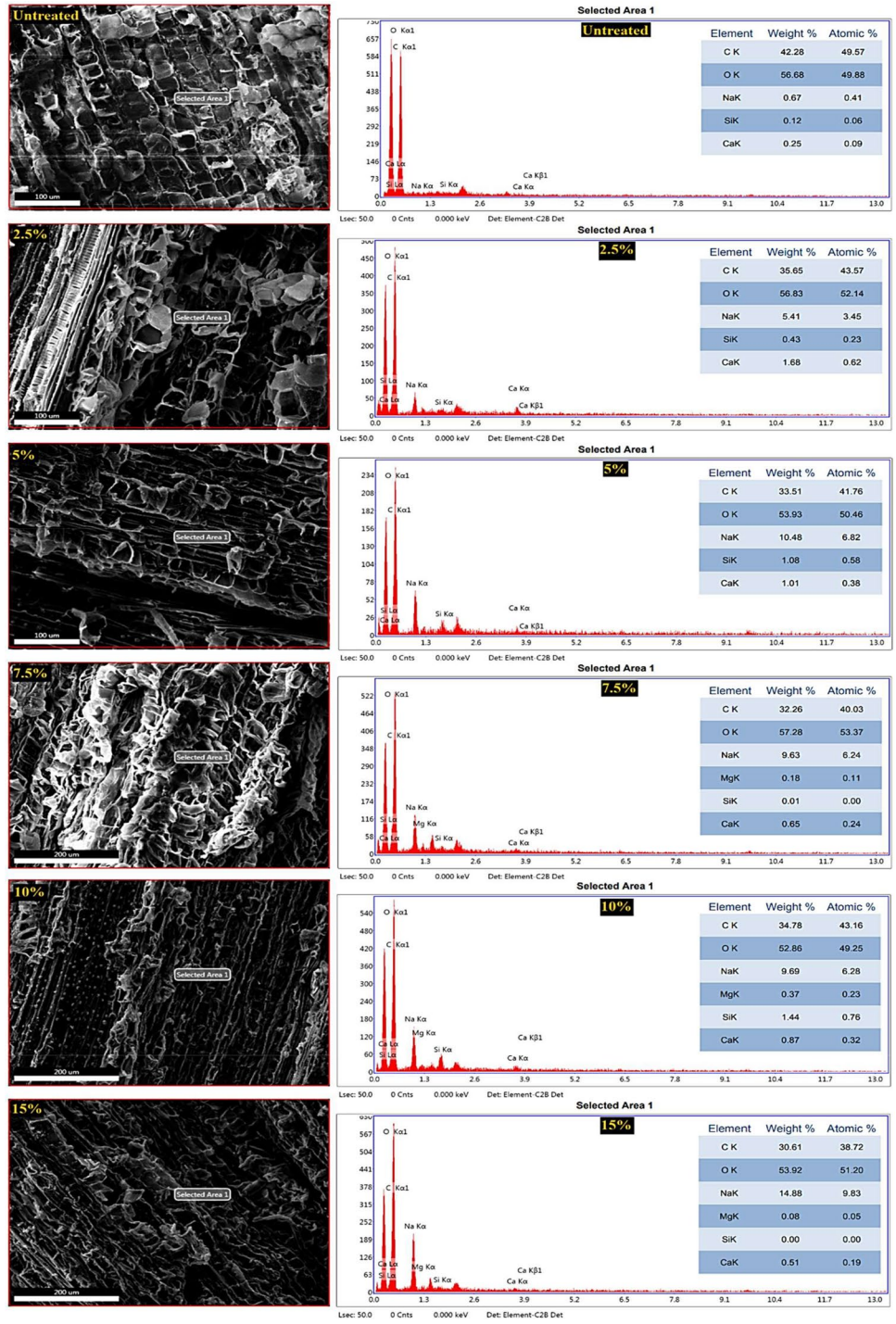
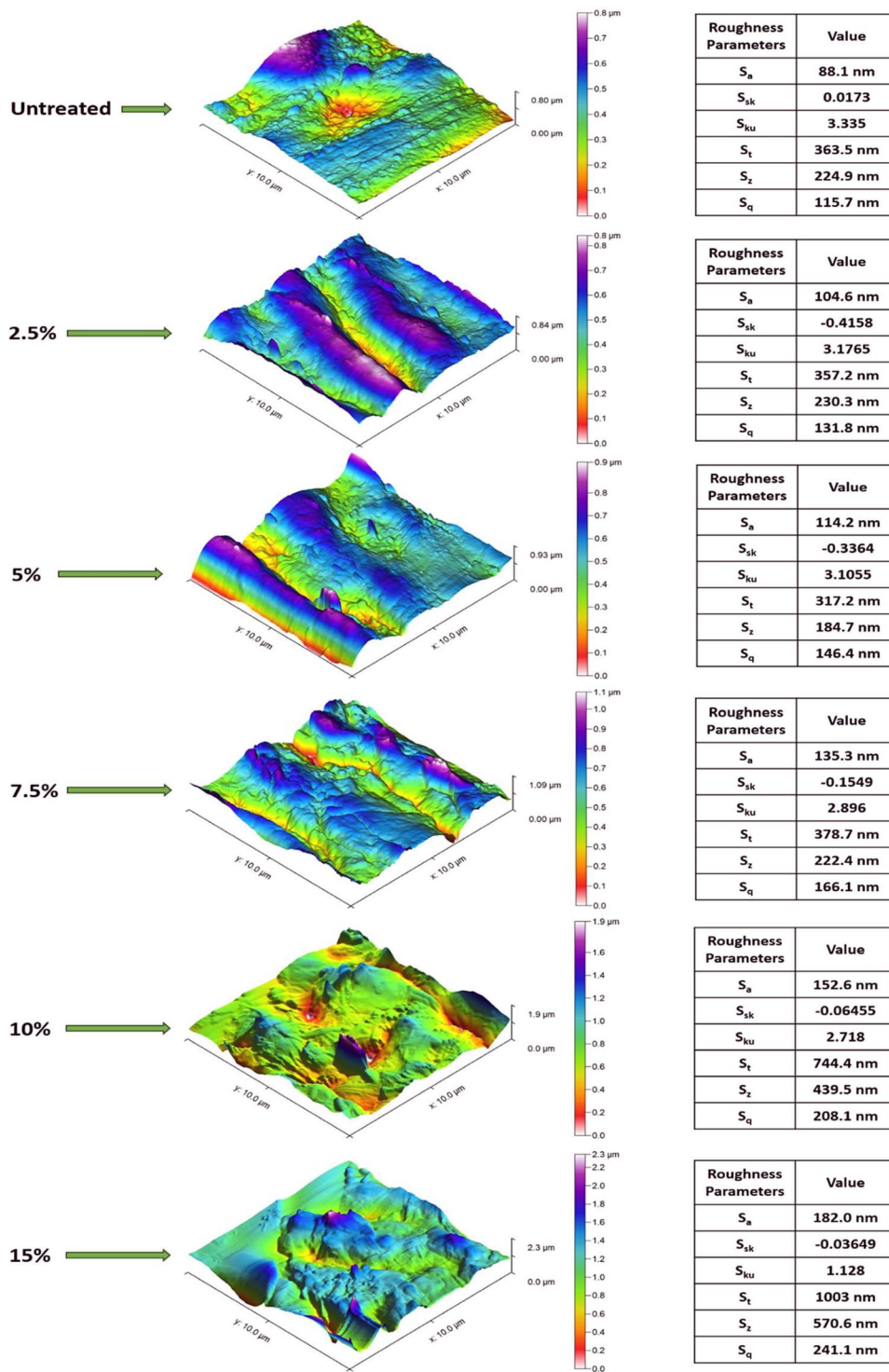


Fig. 8 3D AFM images along with the roughness parameters of alkali-treated and untreated CTCFs



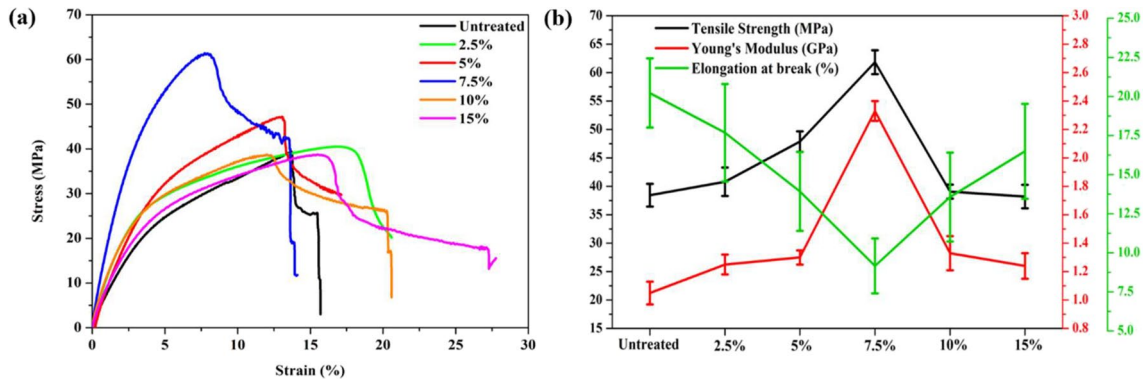


Fig. 9 a Stress–strain curve and b tensile properties of alkali-treated and untreated *Calamus tenuis* canes

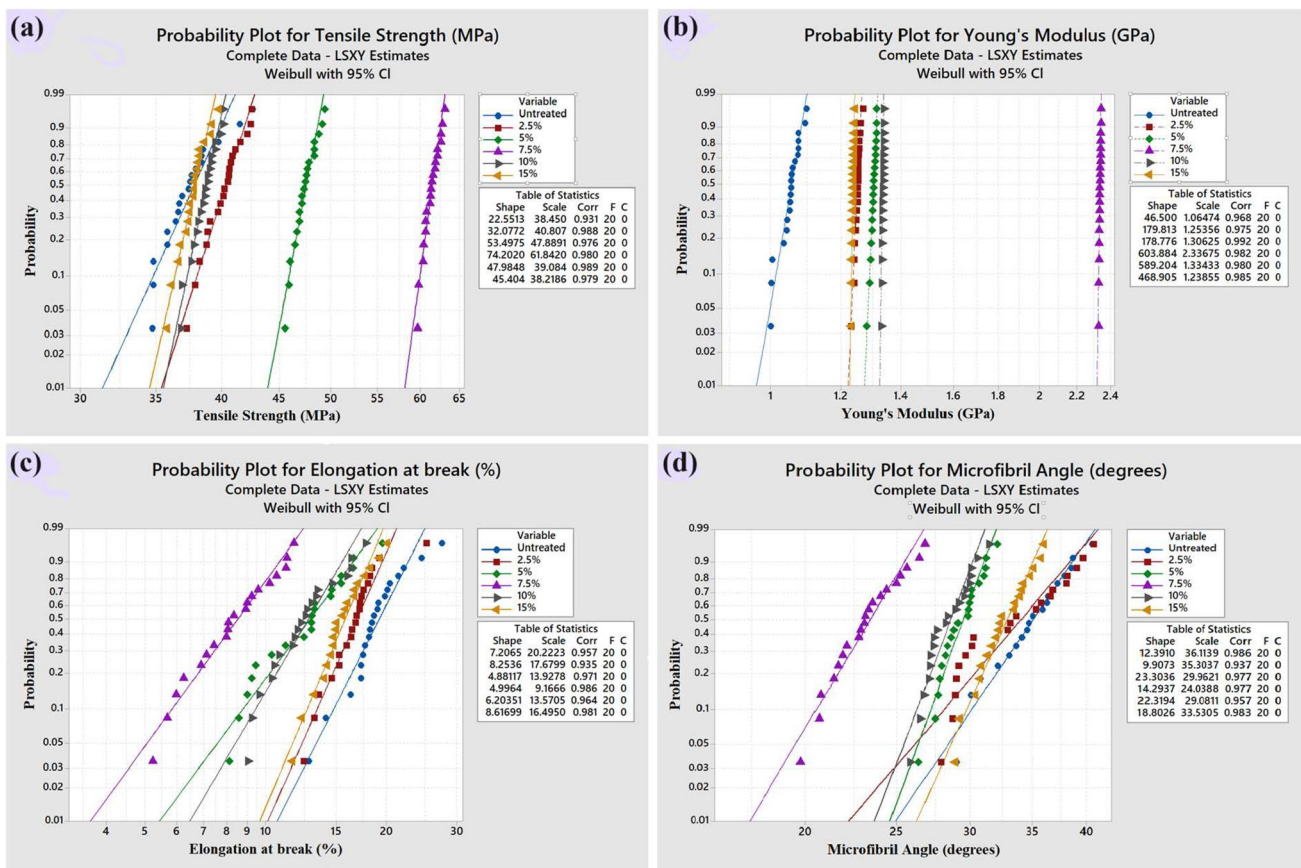


Fig. 10 Weibull distribution plot for a tensile strength, b Young's modulus, c elongation at break, and d microfibril angle of alkali-treated and untreated *Calamus tenuis* canes

Acknowledgements We acknowledge CSIR-NEIST in Jorhat, Assam, for granting us access to their chemical analysis facility. Special thanks are extended to SAIC at Tezpur University for their support with FTIR and SEM, to SAIC at IASST Guwahati for providing AFM facilities, and to SAIF at Gauhati University for access to PXRD and TGA facilities. We also extend our appreciation to CSIC at Dibrugarh University for their valuable contribution to EDX analysis. Finally, we acknowledge Mr. Sanjib Sarma at IIT Guwahati for generously allowing us to utilize their laboratory for conducting tensile tests.

Author contribution Conceptualization: Dip Saikia; methodology: Arup Kar, Dip Saikia; formal analysis and investigation: Arup Kar, Dip Saikia; writing—original draft preparation: Arup Kar; writing—review and editing: Arup Kar, Dip Saikia, Narayanasamy Pandiarajan; resources: Dip Saikia, Narayanasamy Pandiarajan; supervision: Dip Saikia.

Data availability There is no dataset provided with this submission.

Declarations

Ethical approval Not applicable.

Competing interests The authors declare no competing interests.

References

- Xia L, Zhang C, Wang A et al (2020) Morphologies and properties of *Juncus effusus* fiber after alkali treatment. *Cellulose* 27:1909–1920. <https://doi.org/10.1007/s10570-019-02933-9>
- Shanmugasundaram N, Rajendran I, Ramkumar T (2018) Characterization of untreated and alkali treated new cellulosic fiber from an Areca palm leaf stalk as potential reinforcement in polymer composites. *Carbohydr Polym* 195:566–575. <https://doi.org/10.1016/j.carbpol.2018.04.127>
- Sari NH, Sanjay MR, Arpitha GR et al (2019) Synthesis and properties of pandanwangi fiber reinforced polyethylene composites: evaluation of dicumyl peroxide (DCP) effect. *Compos Commun* 15:53–57. <https://doi.org/10.1016/j.coco.2019.06.007>
- Rangappa SM, Siengchin S, Parameswaranpillai J et al (2022) Lignocellulosic fiber reinforced composites: progress, performance, properties, applications, and future perspectives. *Polym Compos* 43:645–691. <https://doi.org/10.1002/pc.26413>
- Jagadeesh P, Puttegowda M, Thyavihalli Girijappa YG et al (2022) Effect of natural filler materials on fiber reinforced hybrid polymer composites: an overview. *J Nat Fibers* 19:4132–4147. <https://doi.org/10.1080/15440478.2020.1854145>
- Sanjay MR, Madhu P, Jawaid M et al (2018) Characterization and properties of natural fiber polymer composites: a comprehensive review. *J Clean Prod* 172:566–581. <https://doi.org/10.1016/j.jclepro.2017.10.101>
- Widodo E, Pratikto S, Widodo TD (2024) Comprehensive investigation of raw and NaOH alkalinized sansevieria fiber for enhancing composite reinforcement. *Case Stud Chem Environ Eng* 9:100546. <https://doi.org/10.1016/j.csee.2023.100546>
- Shibly MAH, Islam MdI, Rahat MdNH et al (2024) Extraction and characterization of a novel cellulosic fiber derived from the bark of *Rosa hybrida* plant. *Int J Biol Macromol* 257:128446. <https://doi.org/10.1016/j.ijbiomac.2023.128446>
- Ovali S (2023) Characterization of lignocellulosic *glycyrrhiza glabra* fibers as a potential reinforcement for polymer composites. *J Thermoplast Compos Mater* 36:4241–4256. <https://doi.org/10.1177/08927057231151928>
- Youbi SBT, Tagne NRS, Harzallah O et al (2022) Effect of alkali and silane treatments on the surface energy and mechanical performances of *Raphia vinifera* fibres. *Ind Crops Prod* 190:115854. <https://doi.org/10.1016/j.indcrop.2022.115854>
- Shahril SM, Ridzuan MJM, Majid MSA et al (2022) Alkali treatment influence on cellulosic fiber from *Furcraea foetida* leaves as potential reinforcement of polymeric composites. *J Mater Res Technol* 19:2567–2583. <https://doi.org/10.1016/j.jmrt.2022.06.002>
- Manimaran P, Senthamaraiannan P, Sanjay MR et al (2018) Study on characterization of *Furcraea foetida* new natural fiber as composite reinforcement for lightweight applications. *Carbohydr Polym* 181:650–658. <https://doi.org/10.1016/j.carbpol.2017.11.099>
- Arul Marcel Moshi A, Ravindran D, Sundara Bharathi SR et al (2020) Characterization of surface-modified natural cellulosic fiber extracted from the root of *Ficus religiosa* tree. *Int J Biol Macromol* 156:997–1006. <https://doi.org/10.1016/j.ijbiomac.2020.04.117>
- Gerald Arul Selvan MT, Binoj JS, Mansingh BB, Baby Sajin JA (2023) Physico-chemical properties of alkali treated cellulosic fibers from fragrant screw pine prop root. *J Nat Fibers* 20:148–161. <https://doi.org/10.1080/15440478.2022.2129897>
- Tenazoa C, Savastano H, Charca S et al (2021) The effect of alkali treatment on chemical and physical properties of ichu and cabuya fibers. *J Nat Fibers* 18:923–936. <https://doi.org/10.1080/15440478.2019.1675211>
- Umashankaran M, Gopalakrishnan S (2021) Effect of sodium hydroxide treatment on physico-chemical, thermal, tensile and surface morphological properties of *Pongamia pinnata* L. bark fiber. *J Nat Fibers* 18:2063–2076. <https://doi.org/10.1080/15440478.2019.1711287>
- Dayo AQ, Zegaoui A, Nizamani AA et al (2018) The influence of different chemical treatments on the hemp fiber/polybenzoxazine based green composites: mechanical, thermal and water absorption properties. *Mater Chem Phys* 217:270–277. <https://doi.org/10.1016/J.MATCHEMPHYS.2018.06.040>
- Ly E, hadji B, Bras J, Sadocco P, et al (2010) Surface functionalization of cellulose by grafting oligoether chains. *Mater Chem Phys* 120:438–445. <https://doi.org/10.1016/J.MATCHEMPHYS.2009.11.032>
- M.R. S, Siengchin S, Parameswaranpillai J, et al (2019) A comprehensive review of techniques for natural fibers as reinforcement in composites: preparation, processing and characterization. *Carbohydr Polym* 207:108–121. <https://doi.org/10.1016/j.carbpol.2018.11.083>
- Baskaran PG, Kathiresan M, Pandiarajan P (2022) Effect of alkali-treatment on structural, thermal, tensile properties of *Dichrostachys cinerea* bark fiber and its composites. *J Nat Fibers* 19:433–449. <https://doi.org/10.1080/15440478.2020.1745123>
- Bezazi A, Boumediri H, Garcia del Pino G et al (2022) Alkali treatment effect on physicochemical and tensile properties of date palm rachis fibers. *J Nat Fibers* 19:3770–3787. <https://doi.org/10.1080/15440478.2020.1848726>
- Rajeshkumar G, Hariharan V, Indran S et al (2021) Influence of sodium hydroxide (NaOH) treatment on mechanical properties and morphological behaviour of phoenix sp. fiber/epoxy composites. *J Polym Environ* 29:765–774. <https://doi.org/10.1007/s10924-020-01921-6>
- Ben Sghaier AEO, Chaabouni Y, Msahli S, Sakli F (2012) Morphological and crystalline characterization of NaOH and NaOCl treated *Agave americana* L. fiber. *Ind Crops Prod* 36:257–266. <https://doi.org/10.1016/j.indcrop.2011.09.012>
- Vijay R, Vinod A, Lenin Singaravelu D et al (2021) Characterization of chemical treated and untreated natural fibers from *Pennisetum orientale* grass- a potential reinforcement for

- lightweight polymeric applications. *Int J Lightweight Mater Manuf* 4:43–49. <https://doi.org/10.1016/j.ijlmm.2020.06.008>
25. Mohammed AA, Bachtiar D, Rejab MRM et al (2018) Effects of KMnO_4 treatment on the flexural, impact, and thermal properties of sugar palm fiber-reinforced thermoplastic polyurethane composites. *JOM* 70:1326–1330. <https://doi.org/10.1007/s11837-018-2869-1>
 26. Palanisamy S, Mayandi K, Dharmalingam S et al (2022) Tensile properties and fracture morphology of *Acacia caesia* bark fibers treated with different alkali concentrations. *J Nat Fibers* 19:11258–11269. <https://doi.org/10.1080/15440478.2021.2022562>
 27. Saravanakumar SS, Kumaravel A, Nagarajan T et al (2013) Characterization of a novel natural cellulosic fiber from *Prosopis juliflora* bark. *Carbohydr Polym* 92:1928–1933. <https://doi.org/10.1016/j.carbpol.2012.11.064>
 28. Negawo TA, Polat Y, Buyuknalçaci FN et al (2019) Mechanical, morphological, structural and dynamic mechanical properties of alkali treated Ensete stem fibers reinforced unsaturated polyester composites. *Compos Struct* 207:589–597. <https://doi.org/10.1016/j.compstruct.2018.09.043>
 29. Abrial H, Gafar MF, Andriyanto H et al (2012) Alkali treatment of screw pine (*Pandanus odoratissimus*) fibers and its effect on unsaturated polyester composites. *Polym Plast Technol Eng* 51:12–18. <https://doi.org/10.1080/03602559.2011.593090>
 30. Jang ES, Kang CW (2019) Changes in gas permeability and pore structure of wood under heat treating temperature conditions. *J Wood Sci* 65. <https://doi.org/10.1186/s10086-019-1815-3>
 31. Park SH, Jang JH, Wistara NJ et al (2018) Anatomical and physical properties of Indonesian bamboos carbonized at different temperatures. *J Korean Wood Sci Technol* 46:656–669. <https://doi.org/10.5658/WOOD.2018.46.6.656>
 32. Kar A, Saikia D (2023) Characterization of new natural cellulosic fiber from *Calamus tenuis* (Jati Bet) cane as a potential reinforcement for polymer composites. *Heliyon* 9. <https://doi.org/10.1016/j.heliyon.2023.e16491>
 33. Dampanaboina L, Yuan N, Mendu V (2021) Estimation of crystalline cellulose content of plant biomass using the Updegraff method. *J Vis Exp*. <https://doi.org/10.3791/62031>
 34. Agu CV, Njoku OU, Chilaka FC, Agbiogwu D, Iloabuchi KV, Ukazu B (2014) Physicochemical properties of lignocellulosic biofibres from South Eastern Nigeria: their suitability for biocomposite technology. *Afr J Biotechnol* 13:2050–2057. <https://doi.org/10.5897/AJB2013.13443>
 35. Segal L, Creely JJ, Martin AE, Conrad CM (1959) An empirical method for estimating the degree of crystallinity of native cellulose using the X-ray diffractometer. *Text Res J* 29:786–794. <https://doi.org/10.1177/004051755902901003>
 36. Farrukh MA, Butt KM, Chong K-K, Chang WS (2019) Photoluminescence emission behavior on the reduced band gap of Fe doping in CeO_2 - SiO_2 nanocomposite and photophysical properties. *J Saudi Chem Soc* 23:561–575. <https://doi.org/10.1016/j.jscs.2018.10.002>
 37. Ding L, Han X, Cao L et al (2022) Characterization of natural fiber from manau rattan (*Calamus manan*) as a potential reinforcement for polymer-based composites. *J Bioresour Bioprod* 7:190–200. <https://doi.org/10.1016/j.jobab.2021.11.002>
 38. Balaji AN, Nagarajan KJ (2017) Characterization of alkali treated and untreated new cellulosic fiber from Saharan aloe vera cactus leaves. *Carbohydr Polym* 174:200–208. <https://doi.org/10.1016/j.carbpol.2017.06.065>
 39. Madhu P, Sanjay MR, Jawaid M et al (2020) A new study on effect of various chemical treatments on *Agave americana* fiber for composite reinforcement: Physico-chemical, thermal, mechanical and morphological properties. *Polym Test* 85:106437. <https://doi.org/10.1016/j.polymertesting.2020.106437>
 40. Ganapathy T, Sathiskumar R, Senthamaraikannan P et al (2019) Characterization of raw and alkali treated new natural cellulosic fibres extracted from the aerial roots of banyan tree. *Int J Biol Macromol* 138:573–581. <https://doi.org/10.1016/j.ijbiomac.2019.07.136>
 41. Babu BG, Princewinston D, Saravanakumar SS et al (2022) Investigation on the physicochemical and mechanical properties of novel alkali-treated *Phaseolus vulgaris* fibers. *J Nat Fibers* 19:770–781. <https://doi.org/10.1080/15440478.2020.1761930>
 42. Pokhriyal M, Rakesh PK, Rangappa SM, Siengchin S (2023) Effect of alkali treatment on novel natural fiber extracted from *Himalayacalamus falconeri* culms for polymer composite applications. *Biomass Convers Biorefin*. <https://doi.org/10.1007/s13399-023-03843-4>
 43. Senthamaraikannan P, Saravanakumar SS (2023) Evaluation of characteristic features of untreated and alkali-treated cellulosic plant fibers from *Mucuna atropurpurea* for polymer composite reinforcement. *Biomass Convers Biorefin*. <https://doi.org/10.1007/s13399-022-03736-y>
 44. Herlina Sari N, Wardana ING, Irawan YS, Siswanto E (2018) Characterization of the chemical, physical, and mechanical properties of NaOH-treated natural cellulosic fibers from corn husks. *J Nat Fibers* 15:545–558. <https://doi.org/10.1080/15440478.2017.1349707>
 45. Kathirselvam M, Kumaravel A, Arthanarieswaran VP, Saravanakumar SS (2019) Characterization of cellulose fibers in *Thespesia populnea* barks: influence of alkali treatment. *Carbohydr Polym* 217:178–189. <https://doi.org/10.1016/j.carbpol.2019.04.063>
 46. Senthamaraikannan P, Kathiresan M (2018) Characterization of raw and alkali treated new natural cellulosic fiber from *Coccinia grandis* L. *Carbohydr Polym* 186:332–343. <https://doi.org/10.1016/j.carbpol.2018.01.072>
 47. Mudoi MP, Sinha S, Parthasarthy V (2022) Optimizing the alkali treatment of cellulosic Himalayan nettle fibre for reinforcement in polymer composites. *Carbohydr Polym* 296. <https://doi.org/10.1016/j.carbpol.2022.119937>
 48. Udhayakumar A, Mayandi K, Nagarajan R et al (2023) Effect of chemical treatment on physico-chemical properties of a novel extracted cellulosic *Cryptostegia grandiflora* fiber. *Mater Res Express*. <https://doi.org/10.1088/2053-1591/ace29c>
 49. Vijay R, Lenin Singaravelu D, Vinod A et al (2019) Characterization of raw and alkali treated new natural cellulosic fibers from *Tridax procumbens*. *Int J Biol Macromol* 125:99–108. <https://doi.org/10.1016/j.ijbiomac.2018.12.056>
 50. Gapsari F, Purnowidodo A, Hidayatullah S, Suteja S (2021) Characterization of Timoho Fiber as a reinforcement in green composite. *J Mater Res Technol* 13:1305–1315. <https://doi.org/10.1016/j.jmrt.2021.05.049>
 51. Tengsuthiwat J, Vinod A, Srisuk R et al (2022) Thermo-mechanical characterization of new natural cellulose fiber from *Zmioculus zamiifolia*. *J Polym Environ* 30:1391–1406. <https://doi.org/10.1007/s10924-021-02284-2>
 52. Saravanakumar SS, Kumaravel A, Nagarajan T, Moorthy IG (2014) Effect of chemical treatments on physicochemical properties of *Prosopis juliflora* fibers. *Int J Polym Anal Char* 19:383–390. <https://doi.org/10.1080/1023666X.2014.903585>
 53. Sivasubramanian P, Kalimuthu M, Palaniappan M et al (2021) Effect of alkali treatment on the properties of *Acacia caesia* bark fibres. *Fibers* 9. <https://doi.org/10.3390/fib9080049>
 54. Loganathan TM, Sultan MTH, Ahsan Q et al (2020) Characterization of alkali treated new cellulosic fibre from *Cyrtostachys renda*. *J Mater Res Technol* 9:3537–3546. <https://doi.org/10.1016/j.jmrt.2020.01.091>
 55. Alshammari BA, Alotaibi MD, Allothman OY et al (2019) A new study on characterization and properties of natural

- fibers obtained from olive tree (*Olea europaea* L.) residues. *J Polym Environ* 27:2334–2340. <https://doi.org/10.1007/s10924-019-01526-8>
56. Selvaraj M, Pannirselvam N, Ravichandran PT et al (2023) Extraction and characterization of a new natural cellulosic fiber from bark of *Ficus carica* plant as potential reinforcement for polymer composites. *J Nat Fibers* 20. <https://doi.org/10.1080/15440478.2023.2194699>
 57. Johny V, Kuriakose Mani A, Palanisamy S et al (2023) Extraction and physico-chemical characterization of pineapple crown leaf fibers (PCLF). *Fibers* 11. <https://doi.org/10.3390/fib11010005>
 58. Sahayaraj AF, Selvan MT, Ramesh M et al (2024) Extraction, purification, and characterization of novel plant fiber from *Tabernaemontana divaricate* stem to use as reinforcement in polymer composites. *Biomass Convers Biorefin*. <https://doi.org/10.1007/s13399-024-05352-4>
 59. Ndazi BS, Karlsson S, Tesha JV, Nyahumwa CW (2007) Chemical and physical modifications of rice husks for use as composite panels. *Compos Part A Appl Sci Manuf* 38:925–935. <https://doi.org/10.1016/j.compositesa.2006.07.004>
 60. Seki Y, Sarikanat M, Sever K, Durmuşkahya C (2013) Extraction and properties of *Ferula communis* (chakshir) fibers as novel reinforcement for composites materials. *Compos B Eng* 44:517–523. <https://doi.org/10.1016/j.compositesb.2012.03.013>
 61. Tamanna TA, Belal SA, Shibly MAH, Khan AN (2021) Characterization of a new natural fiber extracted from *Corypha taliera* fruit. *Sci Rep* 11. <https://doi.org/10.1038/s41598-021-87128-8>
 62. Indran S, Raj RE (2015) Characterization of new natural cellulosic fiber from *Cissus quadrangularis* stem. *Carbohydr Polym* 117:392–399. <https://doi.org/10.1016/j.carbpol.2014.09.072>
 63. Devnani GL, Sinha S (2019) Extraction, characterization and thermal degradation kinetics with activation energy of untreated and alkali treated *Saccharum spontaneum* (Kans grass) fiber. *Compos B Eng* 166:436–445. <https://doi.org/10.1016/j.compositesb.2019.02.042>
 64. Sahayaraj AF, Selvan MT, Jenish I, Ramesh M (2023) Extraction and characterization of novel cellulosic fiber from *Jatropha integerrima* plant stem for potential reinforcement in polymer composites. *Biomass Convers Biorefin*. <https://doi.org/10.1007/s13399-023-04541-x>
 65. Gentil Elenga R, Djemia P, Tingaud D, Chauveau T, Goma Maniongui J, Dirras G (2013) Raffia fiber microstructure.
 66. Hadou A, Belaadi A, Alshahrani H, Khan MKA (2024) Extraction and characterization of novel cellulose fibers from *Draacaena draco* plant. *Mater Chem Phys* 313:128790. <https://doi.org/10.1016/j.matchemphys.2023.128790>
 67. Prithiviraj M, Muralikannan R (2022) Investigation of optimal alkali-treated *Perotis indica* plant fibers on physical, chemical, and morphological properties. *J Nat Fibers* 19:2730–2743. <https://doi.org/10.1080/15440478.2020.1821291>
 68. Ramalingam K, Thiagamani SMK, Pulikkalparambil H et al (2023) Novel cellulosic natural fibers from *Abelmoschus ficulneus* weed: extraction and characterization for potential application in polymer composites. *J Polym Environ* 31:1323–1334. <https://doi.org/10.1007/s10924-022-02687-9>
 69. Chen H, Zhang W, Wang X et al (2018) Effect of alkali treatment on wettability and thermal stability of individual bamboo fibers. *J Wood Sci* 64:398–405. <https://doi.org/10.1007/s10086-018-1713-0>
 70. Kar A, Saikia D, Palanisamy S et al (2023) Effect of alkali treatment under ambient and heated conditions on the physicochemical, structural, morphological, and thermal properties of *Calamus tenuis* cane fibers. *Fibers* 11:92. <https://doi.org/10.3390/fib11110092>
 71. Selvan MT, Jenish I, Ramesh M, Sahayaraj AF (2023) Characterization of *Plumeria pudica* bark fiber for reinforcing lightweight polymer composites and evaluating its physical, chemical, and thermal properties. *Biomass Convers Biorefin*. <https://doi.org/10.1007/s13399-023-05172-y>
 72. Fiore V, Scalici T, Valenza A (2014) Characterization of a new natural fiber from *Arundo donax* L. as potential reinforcement of polymer composites. *Carbohydr Polym* 106:77–83. <https://doi.org/10.1016/j.carbpol.2014.02.016>
 73. Raia RZ, Iwakiri S, Trianoski R, et al (2021) Effects of alkali treatment on modification of the *Pinus fibers*. *Matéria (Rio de Janeiro)* 26. <https://doi.org/10.1590/s1517-707620210001.1236>
 74. Ramasamy R, Obi Reddy K, Varada Rajulu A (2018) Extraction and characterization of *Calotropis gigantea* bast fibers as novel reinforcement for composites materials. *J Nat Fibers* 15:527–538. <https://doi.org/10.1080/15440478.2017.1349019>
 75. Oushabi A, Sair S, Oudrhiri Hassani F et al (2017) The effect of alkali treatment on mechanical, morphological and thermal properties of date palm fibers (DPFs): study of the interface of DPF–polyurethane composite. *S Afr J Chem Eng* 23:116–123. <https://doi.org/10.1016/j.sajce.2017.04.005>
 76. Han X, Ding L, Tian Z, et al (2021) Extraction and characterization of novel ultrastrong and tough natural cellulosic fiber bundles from manau rattan (*Calamus manan*). *Ind Crops Prod* 173. <https://doi.org/10.1016/j.indcrop.2021.114103>
 77. Li J, Ma R, Lu Y et al (2020) A gravity-driven high-flux catalytic filter prepared using a naturally three-dimensional porous rattan biotemplate decorated with Ag nanoparticles. *Green Chem* 22:6846–6854. <https://doi.org/10.1039/D0GC01709D>
 78. Tomlinson PB, Fisher JB, Spangler RE, Richer RA (2001) Stem vascular architecture in the rattan palm *Calamus* (Arecaceae–Calamoideae–Calaminae). *Am J Bot* 88:797–809
 79. Kim JM, Song IS, Cho DH, Hong IP (2011) Effect of carbonization temperature and chemical pre-treatment on the thermal change and fiber morphology of kenaf-based carbon fibers. *Carbon Lett* 12:131–137. <https://doi.org/10.5714/CL.2011.12.3.131>
 80. Verma D, Goh KL (2021) Effect of mercerization/alkali surface treatment of natural fibres and their utilization in polymer composites: mechanical and morphological studies. *J Compos Sci* 5:175. <https://doi.org/10.3390/jcs5070175>
 81. Sahayaraj A F, Muthukrishnan M, Jenish I (2023) Extraction and characterization of sponge gourd outer skin fiber. *J Nat Fibers* 20. <https://doi.org/10.1080/15440478.2023.2208888>
 82. Wirawan WA, Sabitah A, Choiron MA et al (2023) Effect of chemical treatment on the physical and thermal stability of *Hibiscus tiliaceus* bark fiber (HBF) as reinforcement in composite. *Results Eng* 18:101101. <https://doi.org/10.1016/j.rineng.2023.101101>
 83. Saha A, Kumari P (2023) Effect of alkaline treatment on physical, structural, mechanical and thermal properties of *Bambusa tulda* (Northeast Indian species) based sustainable green composites. *Polym Compos* 44:2449–2473. <https://doi.org/10.1002/pc.27256>
 84. Sathishkumar T, Navaneethakrishnan P, Shankar S et al (2013) Characterization of natural fiber and composites – a review. *J Reinf Plast Compos* 32:1457–1476. <https://doi.org/10.1177/0731684413495322>

Publisher's Note Springer Nature remains neutral with regard to jurisdictional claims in published maps and institutional affiliations.

Springer Nature or its licensor (e.g. a society or other partner) holds exclusive rights to this article under a publishing agreement with the author(s) or other rightsholder(s); author self-archiving of the accepted manuscript version of this article is solely governed by the terms of such publishing agreement and applicable law.